Microelectronic Engineering 111 (2013) 242–246

Contents lists available at SciVerse ScienceDirect

Microelectronic Engineering

journal homepage: www.elsevier.com/locate/mee

Optimized ink-jet printing condition for stable and reproducible performance of organic thin film transistor

Dong-Hoon Lee [a], Ki-Tae Lim [a], Eung-Kyu Park [a], Jung-Min Kim [b], Yong-Sang Kim [a,*]

[a] School of Electronic and Electrical Engineering, Sungkyunkwan University, Suwon, Gyeonggi 440-746, Republic of Korea
[b] Materials & Devices Lab., Corporate R&D Institute, Samsung Electro-Mechanics Co. Ltd., Suwon, Gyeonggi 443-743, Republic of Korea

ARTICLE INFO

Article history:
Available online 19 April 2013

Keywords:
Inkjet printing
OTFT
Ag ink
PMMA
Pentacene

ABSTRACT

In this work, we fabricated an electrically stable and reproducible organic thin film transistor (OTFT) by optimizing the electrode printing conditions to avoid the coffee ring effect and the Marangoni effect. The electrodes were printed on substrates with different temperature and line spacing to compare the uniformity of electrode morphology and their electrical performance. The Ag gate electrode was printed on poly (methyl methacrylate) (PMMA) coated glass substrate. As a top contact device, source and drain electrodes were also printed on the pentacene layer. The optimized gate electrode was printed at substrate with a temperature of 30 °C and 30 μm spacing size while the source drain electrodes were printed with 80 μm spacing size at 80 °C. The final devices showed reproducible electrode morphology and electrical properties with a mobility of 0.025 cm^2/V-s, threshold voltage $V_{th} = -5.6$ V and on/off ratio >10^4.

1. Introduction

Organic Thin Film Transistor (OTFT) is very attractive for a varied range of applications such as electronic paper, flexible display, sensors and radio-frequency identification (RFID) tags because of their unique advantages such as light weight, low cost of fabrication, flexibility, and solution process. Solution process signifies two advantages, which are, low temperature and no vacuum process [1–3]. The vacuum process includes photo-lithography, evaporation, chemical vapor deposition (CVD), etc. The weak Van der Waals force enables evaporation of organic molecules to form a bulk layer at low temperature. These advantages open new market of electronics which seems impossible using other processes [4–6]. The TFTs based on inorganic materials such as silicon require processing steps at 300 °C or higher in order to incorporate hydrogen to passivate the dangling bond in the bulk semiconductor and at the semiconductor–dielectric interface [7,8].

However, organic semiconductors can be simply evaporated from a powder at low temperature (under 200 °C) or dissolved in solvent. The solution can be easily patterned using screen or ink-jet printing, while keeping the substrate at near room temperature. The lack of dangling bonds omits the need for high temperature annealing. Therefore, the low temperature processing conditions of OTFT permit them to be fabricated in a wide range of mechanical flexible, low glass transition temperature substrate such as PET or PEN. The ability of organic materials to be dispersed in solvent material enables its use in the solution process. Hence, solution process offers a new paradigm for printed semiconductor fabrication [9,10].

Printed technologies have attracted considerable attention and research such as screen printing, gravure printing, imprinting and ink-jet printing because of physical and chemical vapour deposition are expensive, complicated and inefficient. Among several printing methods, ink-jet printing is a promising technique for electronics because of cost-efficient and precise processing. Additionally, ink-jet printing can be used for patterning every material such as metal, semiconductor, and insulator. Specially, conductive inks are typically used for electronics due to their chemical stability in ambient atmosphere and good electrical conductivity. Hence many researchers are studying ink-jet printing to fabricate TFTs [10,11].

In most cases, although top contact device shows better performance than bottom contact TFT, the process of inkjet-printer has been typically applied to the formation of source/drain electrodes or an active layer in a bottom contact TFT structure. Because there are, in general, limitations of ink-jet printer in reliability, resolution, available material, surface roughness of the ink-jet printed layer and adhesion between ink-jet printed layers [12–14].

The most difficult task for ink-jet printed electrodes is the appearance of coffee ring effect around the periphery of dots and lines. The best inkjet-printed lines should be distinct, smooth, and straight. However, recent works from our group and others investigators felt a need to optimize this behavior of ink-jet printed ink. In printed integrated electronics, the various acts of electrically

* Corresponding author. Tel.: +82 31 299 4323; fax: +82 31 290 5828.
E-mail address: yongsang@skku.edu (Y.-S. Kim).

0167-9317/$ - see front matter © 2013 Elsevier B.V. All rights reserved.
http://dx.doi.org/10.1016/j.mee.2013.03.177

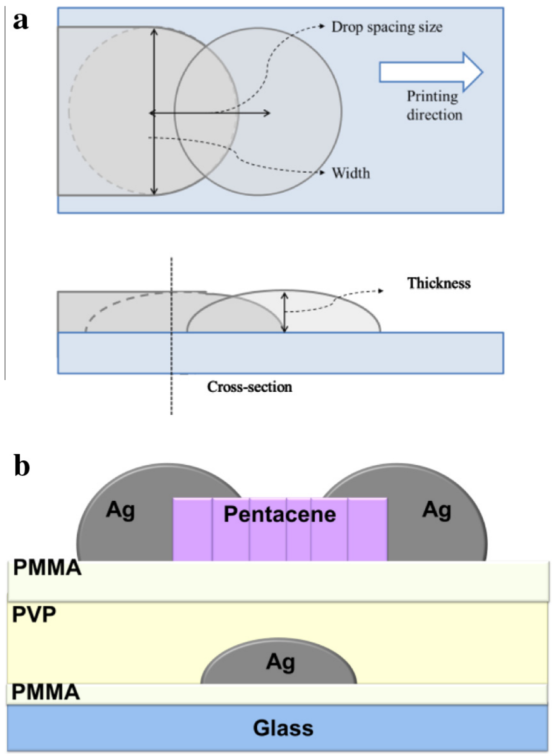

Fig. 1. (a) Mechanism of electrode printing. (b) Cross-sectional view of an OTFTs structure.

active materials cause different engineering constraints. For instance, in a bottom-gated transistor, the gate line must be as flat and as smooth as possible. The source/drain electrode needs sharp edges with a small, controlled separation although their width is less critical. We found that in order to create a straight, predictable line it is equally important to make it distinctive and flat. Researchers have also minimized the coffee ring effect in printed electrodes maintaining its thermal condition on a heated substrate [15]. However, ink-jet printing often shows poor control of uniformity and non-reproducible electrode morphology which lead to instable of electrical performance.

In this paper, to overcome the critical point of ink-jet printing; we report an optimum printing condition to draw gate and source/drain electrode taking into consideration a range of temperatures, line pitch and surface treatment over active layer using HMDS (Hexamethyldisilazane). We studied line morphology with varying temperature and spacing size and optimized the printing conditions of electrode to fabricate an OTFT.

2. Experiment

For this work, we used Ag inks (DGP-40LT-15C) with an Ag content of 40–45 wt.% purchased from ANP Co. and carried out our experiment using an ink-jet printer (OmiJet100, UNIJET Co.). The printer employs a piezoelectric jetting head of 30 pL at a pulse wave form which applies voltage of 82 V during 5 μs with 1 μs for t_{rise} and 1 μs t_{fall}. The head jets 28 pL of ink at a velocity of 1.33 m/s through each nozzle at a frequency of about 1 kHz. We printed the TFT on glass substrate pre-coated with PMMA layer. The size of single dot on PMMA measured around 80 μm.

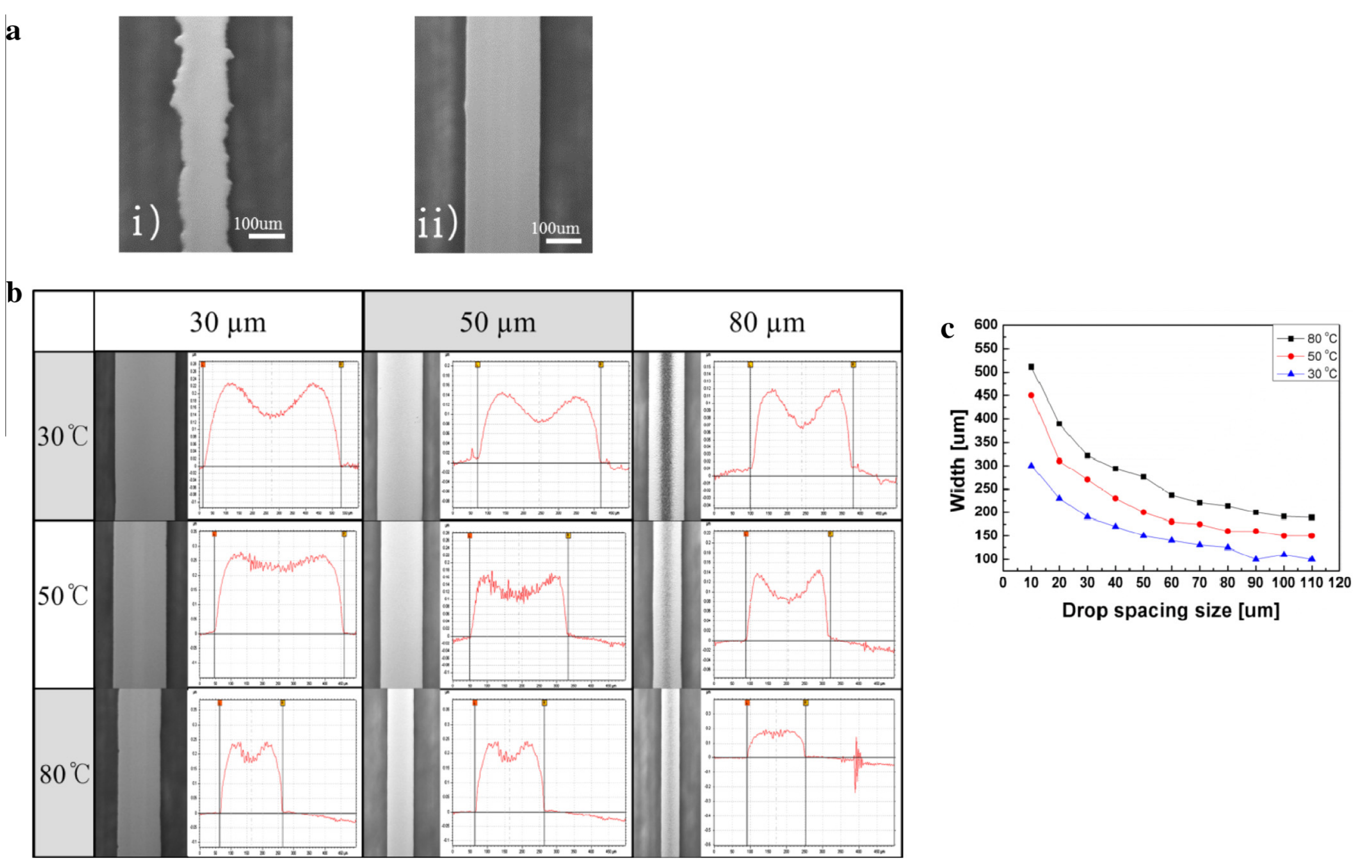

Fig. 2. (a) Printed gate electrode on (i) bare glass and (ii) PMMA coated glass. (b) Alpha steps profile, optical microscope image and (c) width of the printed Ag electrode, dependent on substrate temperature and spacing size.

We fabricated an all inkjet-printed OTFT except for the deposition of active layer and the insulator coating. To optimize the printing condition, of the gate and source/drain electrode, we calibrated the line resolution, substrate temperatures and substrate condition. Fig. 1(a) explains the terms and the mechanism of how thickness and width of dot is measured. Fig. 1(b) shows a cross-section view of the consummate device. The device constitutes of a bare glass substrate that was ultrasonically cleaned with acetone, isopropyl alcohol and deionized water for 20 min respectively. The substrate was then kept in a dry oven for 30 min at 100 °C to remove vestigial solvent or particles from the substrate. PMMA was then spin-coated at 4500 RPM for 60 s over bare glass and baked at 160 °C for 30 min in a conventional oven. We then printed electrode line of similar dimension with variable condition such as drop spacing and substrate temperature using Ag ink. On the top of the gate electrode, poly 4-vinyl phenol (PVP) (Sigma, 10 wt.%) was spin-coated to a thickness of 300 nm and thermally cured. 10 wt.% PVP solution was mixed with CLA- ply (melamine-co-formaldehyde) (Sigma, 5 wt.%) in PGMEA solvent. PMMA (Sigma, 4 wt.% in anisole) was then spin-coated to a thickness of 180 nm on PVP layer and cured in the conventional oven. The pentacene active layer was patterned through the shadow mask by thermal evaporation at a rate of 0.1 Å/s to a thickness of about 70 nm at fixed 85 °C. Pentacene evaporated device was treated with HMDS for surface coating which prevents Ag ink to snuggle into pentacene. HMDS was spin coated at 4500 rpm for 35 s and dried at room temperature. After treating the surface, the source and drain electrodes, an Ag layer were printed by ink-jet printer. The channel length (L) and width (W) were 70 μm and 1000 μm, respectively. The output and transfer characteristic curve of the manufactured device was measured using Keithley 236.

3. Result & discussion

To investigate the printing condition for uniform fabrication, we first printed an Ag electrode on the bare glass substrate. Fig. 2(a) (i) shows the shape of the ink-jet printed electrode on the bare glass substrate. Due to the circulation of ink, budding of electrode can be seen at the edges. The electrode also showed in-stable condition due to coffee ring effect and Marangoni effect. To prevent these effects, we printed gate electrode on a PMMA coated glass substrate which is shown in Fig. 2(a) (ii). Because PMMA has a stable surface energy, coating of it on the substrate resulted in a uniform electrode boundary. Spin coating of PMMA decreased the contact angle of Ag ink on the substrate leading to a better result. To optimize the condition of the electrode, we also controlled temperature and spacing size between two lines ranging from 30 μm to 80 μm during printing. The temperature of the substrate varied from 30 °C to 80 °C. Fig. 2(b) shows the alpha-step profile and the optical microscope image of the printed electrodes at different substrate temperature with different line spacing. And Fig. 2(c) shows thickness and width of electrode with varied condition. Width of the gate electrode exponentially increased when the temperature decreased. And the surface of the electrode becomes smoother when temperature and spacing size decreases. These effects are the results of different evaporation speed of solvent and particle flow speed. Drop spacing and substrate temperature have an influence on total evaporation time and particle flow speed [16]. The coffee ring effect occurs at low temperature because Ag particle has enough time to move towards the edge. Drop spacing also affects the time of evaporation as the total volume of ink increased. Smooth surface can be formed at low temperature and narrow spacing size with enough evaporation time.

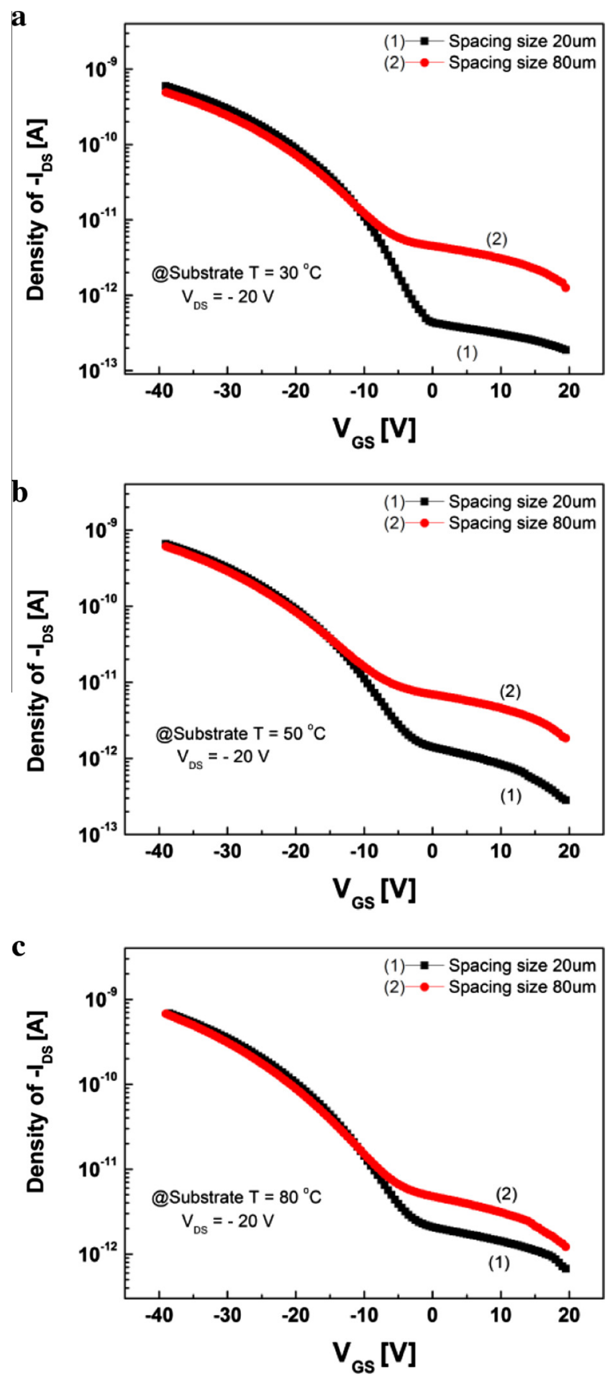

Fig. 3. Transfer property of OTFT with varied spacing size of ink-jet printed gate electrode. (Substrate T = (a) 30 °C, (b) 50 °C, (c) 80 °C).

Transfer curve of all the OTFT devices fabricated at different substrate temperature and spacing size is shown in Fig. 3 for comparison. All the devices have same length but different width. Despite of coffee ring effect, low temperature and large spacing size condition showed best performance from the point of view of off-current state due to smooth surface condition. Finally, we settled to an optimized condition of 30 μm spacing size with a substrate temperature of 30 °C for gate electrode printing.

After optimizing gate electrode, we deposited pentacene layer on varied insulator surface, which was spin-coated to control the size of grain boundary. Commonly, PVP layer can make larger

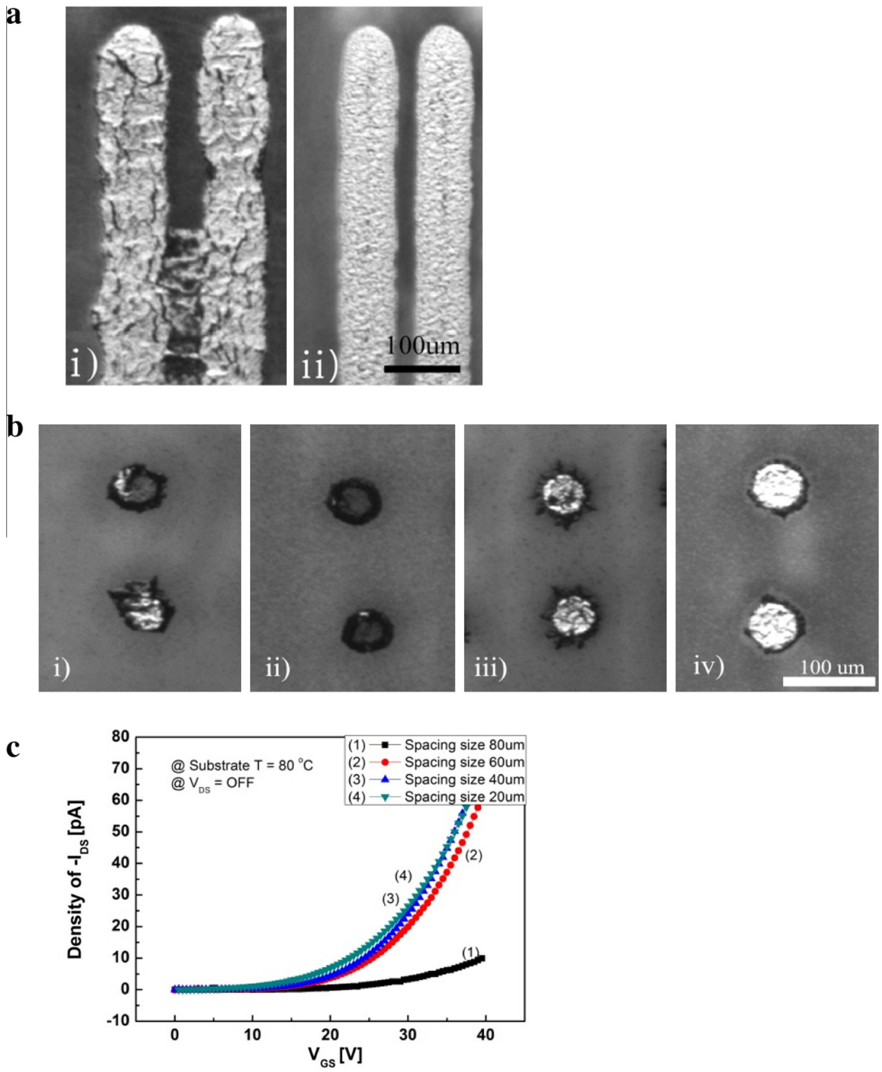

Fig. 4. (a) Printed line on the pentacene surface with different insulator (i) PVP, (ii) PMMA. (b) Printed dot on the pentacene surface with different temperature (i) 30 °C, (ii) 50 °C, (iii) 80 °C. (c) Source and drain leakage current characteristic dependent on spacing size.

grain boundary size than PMMA layer. Large grain boundary has a detrimental effect on the printing condition. Fig. 4(a) shows the result of line morphologies on different grain boundary condition. As you can see, large grain boundary of pentacene on PVP brings about overflow through boundary valley. But, only PMMA layer is too thin which can short gate electrode. Therefore, we used double insulator layer to fabricate OTFT. We deposited pentacene layer after spin-coating PVP-PMMA double layer followed by surface treatment of pentacene layer using HMDS. Because HMDS can change hydrophilic surface to hydrophobic, it prevents soak up of Ag-ink and print more clear & reproducible electrode.

After optimizing the surface condition, we first tried to standardize the substrate temperature to print the source/drain electrode on pentacene. We printed dot using ink-jet printer on the pentacene with different substrate temperature. Fig. 4(b) shows optical image of printed dot with different substrate temperature. High temperature with HMDS treatment shows best stable shape. The other condition deteriorated the device morphology leading to an unstable electrical results. Because Ag ink can soak into the grain boundary and cause a short circuit between source and drain, Ag ink should be dried and pinned as soon as possible.

Fig. 4(c) shows leakage current of source/drain electrode with V_{GS} = OFF. Narrow spacing size shows higher leakage current at source-drain which occurred due to conductivity change of pentacene. Because of narrow spacing of ink, level of total ink volume increases which can overflow and attack the pentacene. For this reason, we settled an optimized conditions which are high temperature of 80 °C and spacing size of 80 μm with HMDS treatment for source drain electrode.

Finally we demonstrate an optimized OTFT which has a gate electrode printed at 30 °C substrate temperature with 10 μm spacing size and source drain electrode printed with 80 μm spacing size at 80 μm. Fig. 5(a) and (b) shows output and transfer graph of optimized OTFT with optical image of device. This OTFT has a 70 μm length and 1000 μm width. The performance of OTFT, $\mu = 0.025\ cm^2/V\text{-}s$, $V_T = -5.6$ V and on/off current ratio of $>10^4$. And Fig. 5(c) shows reproducible performance of devices realized using ink-jet printing.

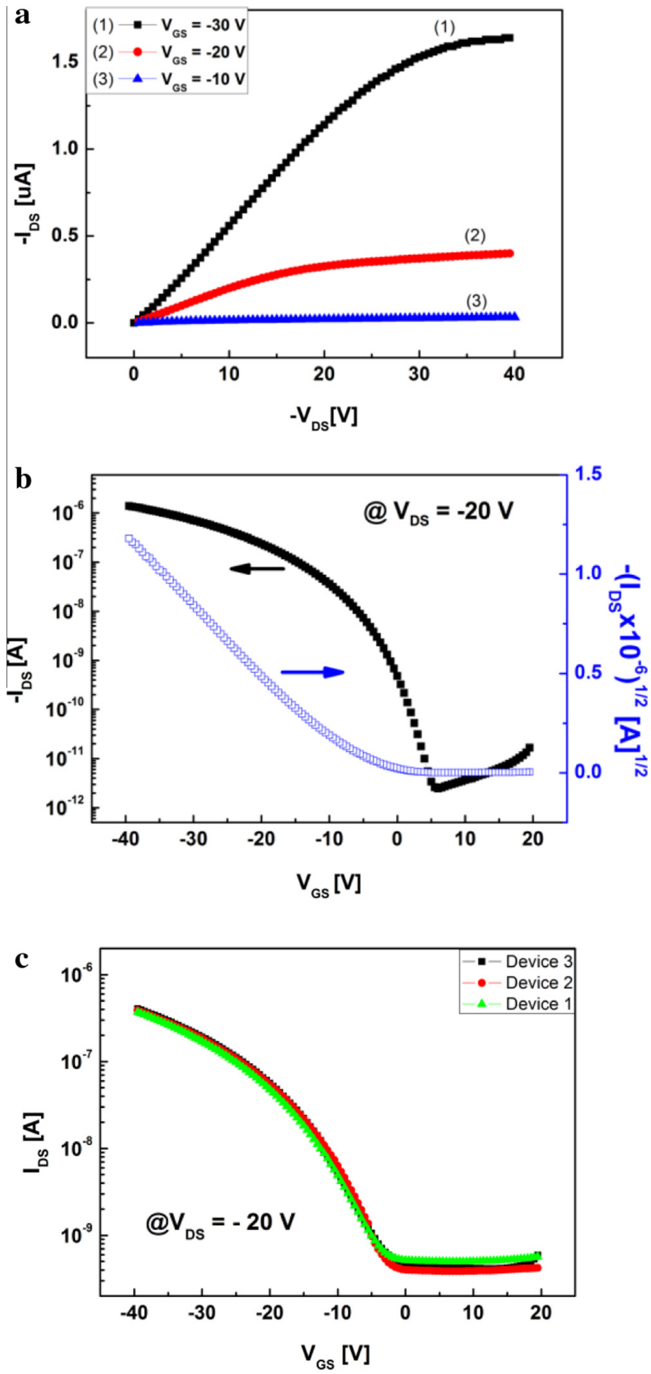

Fig. 5. Electrical properties of ink-jet printed OTFT, (a) output characteristic and (b) transfer characteristic curve. And (c) transfer characteristic curve of reproducible device.

4. Conclusion

We optimized the printing condition to fabricate OTFT using ink-jet printer. Ag gate and source/drain electrodes were printed with stable condition. Optimized printing conditions were 30 °C substrate temperature with 30 μm spacing size for gate electrode and 80 °C substrate temperature with 80 μm spacing size for source-drain electrode with HMDS surface treatment. The device showed stable and reproducible electrode morphology and electrical properties. Device has an electrical mobility of 0.025 cm^2/V-s, threshold voltage $V_{th} = -5.6$ V and on/off ratio >10^4. A further detailed study to fabricate an all-ink-jet printed OTFT and its application would increase the dimension of this research.

References

[1] J. Doggart, Y. Wu, S. Zhu, Appl. Phys. Lett. 94 (2010) 163503–163506.
[2] D. Soltman, V. Subramanian, Langmuir 24 (2008) 2224–2231.
[3] M.Y. Lee, M.W. Lee, J.S. Park, C.K. Song, Microelectron. Eng. 87 (2010) 2577–2581.
[4] K.D. dung, Y.C. Kim, H.C. Shin, B.G. Park, J.D. Lee, E.S. Cho, S.J. Kwon, Appl. Phys. Lett. 96 (2010) 103305.
[5] Y. Yun, C. Pearson, M.C. Petty, J. Appl. Phys. 105 (2009) 034508.
[6] E.V. Tsiper, Z.G. Soos, Phys. Rev. Lett. B 68 (2003) 085031.
[7] D.J. Gundlah, Y.Y. Limm, T.N. Jackson, S.F. Nelson, D.G. Schlom, IEEE Electron Dev. Lett. 80 (2002) 1088.
[8] C.D. Sheraw, L. Zhou, J.R. Huang, D.J. Cundlach, T.N. Jackson, M.G. Kane, I. Hill, Appl. Phys. Lett. 80 (2002) 1800.
[9] H. Sirringhaus, T. Kawase, R.H. Friend, T. Shimoda, E.P. Woo, Science 290 (2000) 2123.
[10] S.-H. Ko, H. Pan, C.P. Grigoropoulos, C.K. Luscombe, J.M.J. Fréchet, D. Poulikakos, Nanotechnology 18 (2007) 345202.
[11] D. Kim, S.-H. Lee, S. Jeong, J. Moon, Electrochem. Solid-State Lett. 12 (2009) H195.
[12] S.-H. Lee, M.-H. Choi, S.-H. Han, D.-J. Choo, J. Jang, S.K. Kwon, Org. Electron. 9 (2008) 721.
[13] J. Doggart, Y. Wu, S. Zhu, Appl. Phys. Lett. 94 (2009) 163503.
[14] S. Gamerith, A. Klug, H. Scheiber, U. Scherf, E. Moderegger, E.J.W. List, Adv. Funct. Mater. 17 (2007) 3111.
[15] D. Soltman, V. Subramanian, Langmuir 24 (2008) 2224.
[16] J.H. Park, J.H. Moon, Langmuir 22 (2006) 3506–3513.